Single-Event Transients in Readout Circuitries at Low Temperature Down to 50 K

Ahmad Al Youssef, Laurent Artola, Samuel Ducret, Guillaume Hubert, Raphael Buiron, Christian Poivey, Franck Perrier, S. Parola

Single Event Transients in Readout circuitries at Low Temperature down to 50K

A. Al Youssef, L. Artola, S. Ducret, G. Hubert, R. Buiron, C. Poivey, F. Perrier, S. Parola

***Abstract* -This paper presents the impact of cryogenic temperatures, down to 50K, on the SET sensitivity of two readout circuit of infrared image sensor designed by Sofradir. Experimental SETs data obtained under heavy ions at the UCL facility are described and the temperature impact on the SET cross sections is presented. The analysis of experimental sensitivity trends is completed by means of MUSCA SEP3 tool.**

***Index Terms*—Single event transient, heavy ions, infrared image sensors, low temperatures, ROIC.**

I. Introduction

Infrared image sensors are used in many space applications [1]. The readout integrated circuitries (ROIC) of infrared sensors are based on CMOS technology. By the way, the digital CMOS circuitries of image sensors are known to be sensitive to single event effects (SEE) [1] [2]. Wherefore, Single-Event (SE) vulnerability in electronics parts has become a major constraint for space applications whatever the temperature conditions. Single-Event induced by the radiation environment in ICs at elevated temperatures (especially in Earth's orbits), from 200K up to 420K, are widely investigated [3]-[5]. However, infrared image sensors are used at very low temperatures (<200K) [6], in order to reduce the dark current and to increase performances.

The goal of this paper is to study the SET sensitivity of two ROICs (ReadOut Integrated Circuit) for a temperature range from 50K up to 300K. The signature (duration, multiplicity and occurrence location) of measured SETs is investigated. This work is based on the analysis of irradiation data obtained under a heavy ions beam at the heavy ion facility based at Université Catholique de Louvain la Neuve, in Louvain la Neuve, Belgium.

The first section of this work presents the ROIC devices tested during the SEE campaign. Two ROICs were developed by Sofradir for near infrared (NIR) and infrared applications (IR) for this campaign. The experimental setup used during the heavy ion irradiations will be also presented in this section. The second section presents the experimental data under heavy ion beams. Finally, this work is completed by simulations with the aim to confirm the assumptions presented in the discussion of experimental results. The simulation work is based on the use of a Monte Carlo SEE prediction tool called MUSCA SEP3. This tool allows for providing SEE estimations and analysis by mean of a simulation flow based on physical and electrical simulations, as presented in previous works [7]–[8].

A. Al Youssef, L. Artola, G. Hubert, are with The French Aerospace Lab (ONERA), Toulouse, France (email: ahmad.al_youssef@onera.fr)
A. Al Youssef, S. Ducret, F. Perrier, S. Parola, R. Buiron are with infrared detectors company (Sofradir), Grenoble, France
C. Poivey is with ESA, ESTEC, 2200 AG Noordwijk ZH the Netherlands

II. Description of SEE Irradiation campaign

A. Devices under Tests

The experimental SEE test vehicle was developed by Sofradir and includes two types of ROIC, as presented in Table I. The first ROIC will be called A in the paper. Two samples ("A1", "A3") of the ROIC A have been tested. ROIC A contains three pixel arrays corresponding to three spectral bands. The dimensions of the first and second arrays are 224 x 4 pixels (line x column). The third array is designed with 448 x 4 pixels table.

The second ROIC is called B. Two samples ("B1", "B2"), have been tested. This ROIC controls also three pixels arrays. The dimensions of the first pixels array is 224 x 8 (Line x column). The second and third arrays are design with a 112 x 4 pixel table.

As mentioned, the two readout circuits have been developed by Sofradir and work at 5V. During the whole SEE tests, the ROIC and its pixel tables are under the heavy ion beams. The results only characterize the silicon system (bare ROIC without MCT attached).

TABLE I
Description of tested ROIC

Device	Part number	Supply voltage	Pixel arrays dimensions
ROIC "A"	Sample "A1", Sample "A3"	5V	2*(224 x 4) 1*(448 x 4)
ROIC "B"	Sample "B1", Sample "B2"	5V	1*(224 x 8) 2*(112 x 4)

B. Experimental Setup during Heavy ions Irradiations

SEE test campaign has been performed at UCL (Université Catholique de Louvain la Neuve) with the heavy ion test facility in Louvain la Neuve, Belgium. Two "Ion cocktails", named MeV/nucl. 5 and MeV/nucl. 3.3 are available in this facility [6]. The heavy ion species are summarized in Table II and Table III.

During all measurements (performed by Sofradir), the temperature of the chip was monitored and regulated, by means of an equipment developed by Sofradir. This cooling equipment maintains the temperature of the DUT to a regulated range of temperature from 50K to 293K. During

each irradiation run a GUARD (Graphical Universal Auto Range Delatcher) system has been used on the DUT's power in order to detect SEL and to prevent its destruction [6]. The occurrences of SETs and SEFI have been detected and recorded during the test campaigns. However, no SEL has been measured during the campaign. The immunity of Sodrafir designs and technology against SEL has been analyzed in a previous work [9].

TABLE II
UCL Ions Cocktail MeV/nucl. 5

Ion	Energie (MeV)	Range (µm(Si))	LET ($MeV.cm^2.mg^{-1}$)
$^{15}N^{3+}$	60	59	3.3
$^{20}Ne^{4+}$	78	45	6.4
$^{40}Ar^{8+}$	151	40	15.9
$^{84}Kr^{17+}$	305	39	40.4
$^{124}Xe^{25+}$	420	37	67.7

TABLE III
UCL Ions Cocktail MeV/nucl. 3.3

Ion	Energie (MeV)	Range (µm(Si))	LET ($MeV.cm^2.mg^{-1}$)
$^{13}C^{4+}$	131	292	1.1
$^{22}Ne^{7+}$	235	216	3
$^{40}Ar^{12+}$	372	117	10.2
$^{58}Ni^{18+}$	567	100	20.4
$^{83}Kr^{25+}$	756	92	32.6

In this paper, only SET cross sections will be presented. Experimental SET test vehicle contains two counters to record SETs. Short SET events are considered when the event duration corresponds to one video frame. Large SET events are considered when the event duration corresponds to two or more video frames, as presented in Table IV. Each short SET and large SET events are recorded in a registers of 30 bits. On the other hand, the measured SEFI events are presented and discussed in a dedicated paper [10].

TABLE IV
Description of SET categories

SET type	Duration of event	SET category	
		Single	Multiple
Short SET	One frame	Only one pixel impacted	Two up to four impacted pixels
Large SET	Two or more frames	Only one pixel impacted	Two up to four impacted pixels

After this description of the experimental setup and the DUT characteristics, the experimental SET data will be presented in the next section.

III. Experimental Data

In this section, experimental cross sections are presented as a function of LET (Linear Energy Transfer), and for a temperature range from 50K up to 300K. As mentioned previously, SETs are separated into two categories described in Table IV: (a) single SETs detected correspond to an event which occurs only on one pixel (b) Multiple SETs correspond to several SETs detected (from two up to four SETs) which occur at least on two pixels. The total SET cross section has been also estimated. This total SET cross section corresponds to the sum of the two SET categories but also the SET events with the events number is higher than 4 but lower than the size of the column of the pixel table.

A. Impact of Cryogenic Temperatures on Large SETs Sensitivity Under Heavy Ion Irradiations

Fig. 1 and Fig. 2 present the large SET cross sections measured on one sample of the readout devices "A" and "B", respectively the samples A1 and B1. The total large SET cross section (black triangles), the large multiple SET (red squares) and the large single SET (blue diamonds) have been measured for a heavy ion with a LET of about $32MeV.cm^2.mg^{-1}$ and for a range of temperatures from 50K up to 293K. The large multiple SETs cross sections are one decade lower than the large single SETs cross. Error bars were calculated and plotted for each cross section value. The statistical errors are very low because of the large events counts.

Fig. 3 and Fig. 4 present the short SET cross sections measured on one sample of the readout devices "A" and "B", respectively the samples A1 and B1. The total short SET cross section (black triangles), the short multiple SETs (red squares) and the short single SETs (blue diamonds) have been calculated for a heavy ion with a LET of about $32MeV.cm^2.mg^{-1}$ and for a range of temperatures from 50K up to 293K. Note that short multiple SETs have been detected only for sample ''A1'' at 55K. This point is discussed in section III.B. Total SETs cross sections are very close to short single SETs cross sections. It means that, the occurrence probability of complex short SET events is very low. As previously, error bars were calculated and plotted for each value of cross section. The statistical errors are very low because of the large events counts.

The results highlight a limited temperature dependence of large and short SETs susceptibilities for the two ROICs. This trend is in good agreement with a previous work done on D- Flip Flop CMOS device, i.e., for temperatures down to 77 K [6]. This limited impact temperature has been highlighted in CMOS gates due to two reasons [5]: (a) saturation of carrier mobility and (b) transistors threshold voltage [11], [12]. The upset of the D-flip flop cell mainly depends on the temperature dependence of the threshold voltage of n-MOS and p-MOS transistor. However, because

of the saturation of the carrier mobility variation, at low temperatures, the variation of the threshold voltage of n-MOS and p-MOS transistors is the same and constant [11].

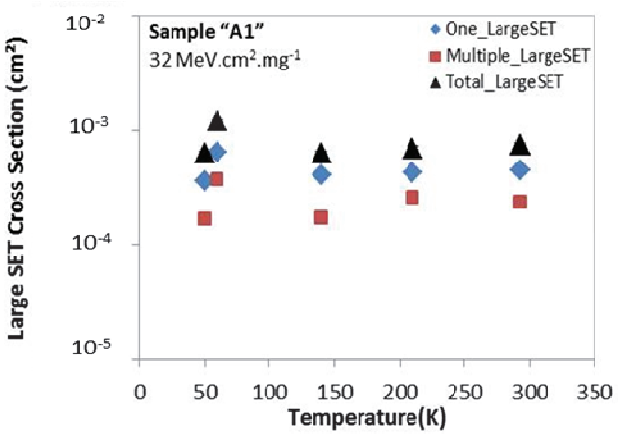

Fig. 1. Large SET experimental cross sections measured on the sample "A1" during the test campaign under heavy ion (32 MeV.cm^2.mg^{-1}), as a function of temperature from 50K to 293K.

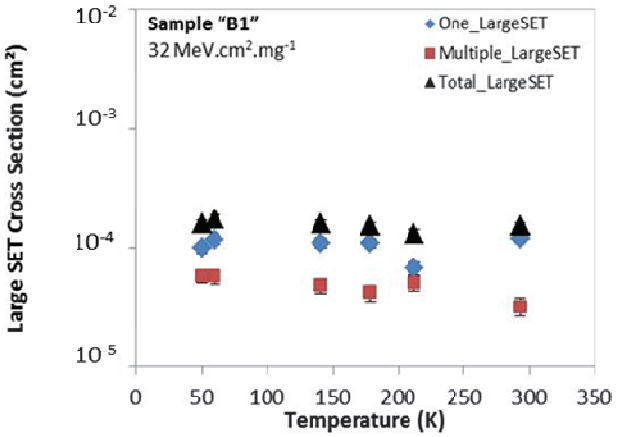

Fig. 2. Large SET experimental cross sections measured on the sample "B1" during the test campaign under heavy ion (32 MeV.cm^2.mg^{-1}), as a function of temperature from 50K to 293K.

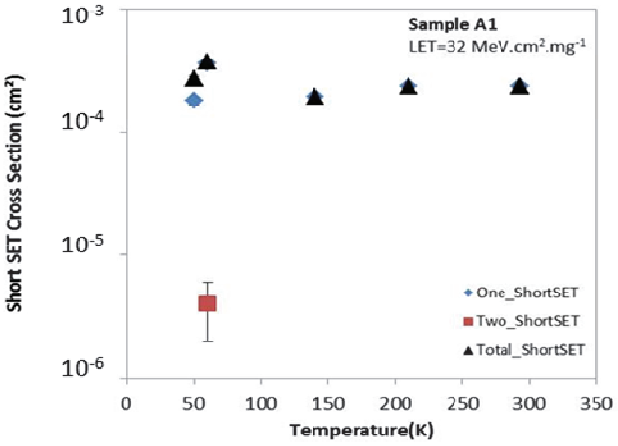

Fig. 3. Short SET experimental cross sections measured on the sample "A1" during the test campaign under heavy ion (32 MeV.cm^2.mg^{-1}), as a function of temperature from 50K to 293K.

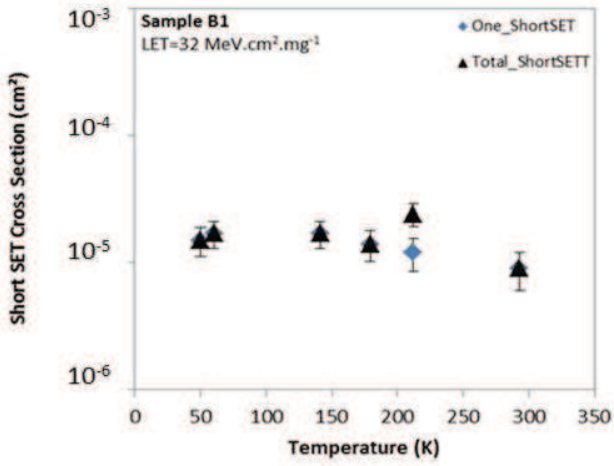

Fig. 4. Short SET experimental cross sections measured on the sample "B1" during the test campaign under heavy ion (32 MeV.cm^2.mg^{-1}), as a function of temperature from 50K to 293K.

B. Short SET Measurements under Heavy Ion Irradiations at 60K

As presented in Section II.B, the short SETs have been detected when a change of pixel level occurs during only one video frame.

Fig. 5 and Fig. 6 present the short SET cross sections measured on two samples of ROIC A: the sample "A1" and sample "A3". The total short SET cross section (black triangles), the short multiple SET (red squares) and the short single SET (blue diamonds) have been calculated during the campaign at 60K for a range of LETs from 3.3MeV.cm^2.mg^{-1} to 67MeV.cm^2.mg^{-1}. Error bars were calculated and plotted for each value of cross section. As shown in Fig. 5, the short SET cross section measured on the sample "A1" increases as a function of LET and saturates above 32MeV.cm^2.mg^{-1}.

The short multiple SET cross sections are two decades lower than the short single SETs cross sections. Same trends are validated in Fig. 6 with sample "A3" of the ROIC "A". Short multiple SET cross sections trends show a low occurrence of short multiple SET as presented in Fig. 3, Fig. 5 and Fig.6. The reason for having few multiple short SET seems to be coherent because the probability of short SET on a pixel causes other short SETs on adjacent pixels is very small. This observation is more discussed in section IV. The results highlight limited impact of the part to part variability in the same lot on the occurrence of short SETs susceptibility at cryogenic temperature for the ROIC "A".

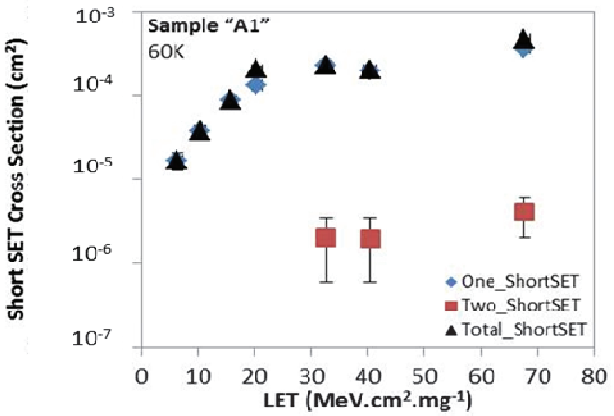

Fig. 5. Short SET experimental cross section measured on the sample "A1" during the test campaign, as a function of LET at 60K.

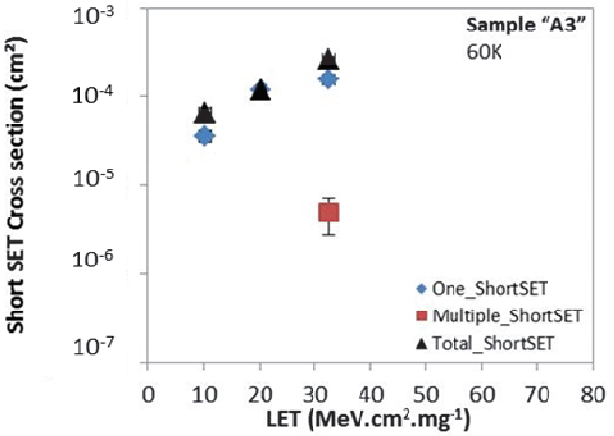

Fig. 6. Short SET experimental cross section measured on the sample "A3" during the test campaign, as a function of LET at 60K.

C. Large SET Measurements under Heavy Ion Irradiations at 60K

As presented in Section II.B, the large SETs have been detected when a change of pixel level occurs during two video frames or longer.

Figs. 7, 8, 9, and 10 present the large SET cross sections calculated from experiments for the samples "A1", "A3", ''B1'' and ''B2" respectively. The total large SET (black triangles), the large multiple SET (red squares) and the large single SET (blue diamonds) cross sections have been calculated during the campaign at 60K for a range of LETs from 3.3MeV.cm^2.mg^{-1} to 67MeV.cm^2.mg^{-1}. As observed previously, the error bars were calculated and plotted for each cross section value. As shown in Fig. 7, the large SET cross sections increase as a function of LET and saturate above 32MeV.cm^2.mg^{-1}. The large multiple SET (red squares) and single SET (blue diamonds) trends in Fig. 7 and Fig. 8 are very close and more significant compared with multiple short SET in Fig. 5 and Fig.6. It means that, the large multiple SET susceptibility is higher than short multiple SET susceptibility. However, the large multiple SET susceptibility (red squares) is 80% lower than the large single SET susceptibility (blue diamonds) of the ROIC "B" as highlighted in Fig. 9. Sample "B1" is less sensitive to large SETs than sample "A1". Same trends are observed in Fig. 10 for the sample "B2" of the ROIC "B".

On the other hand, the total large cross sections of samples "A1", "A3" of ROIC "A" and "B1", "B2" of ROIC "B" are dressed together in Fig. 11 as a function of LET in order to identify two points: (a) the impact of part to part variability in the same lot on the occurrence of large SET susceptibility at cryogenic temperatures for the ROICs "A" and ''B'' and (b) the SET sensitivity comparison between ROIC "A" and "B". the results highlight a limited impact of the part to part in the same lot variability in three points of ROIC "B", and a very limited impact of part to part variability between "A1", "A3".

For most points in Fig. 11, ROIC "B" is less sensitive to large SET than ROIC "A". This refers to the difference in design between ROIC "A" and "B". ROIC "B" has a pitch (distance between two pixels) twice as large as that of ROIC "A". All design elements are not available due to commercial sensitivities.

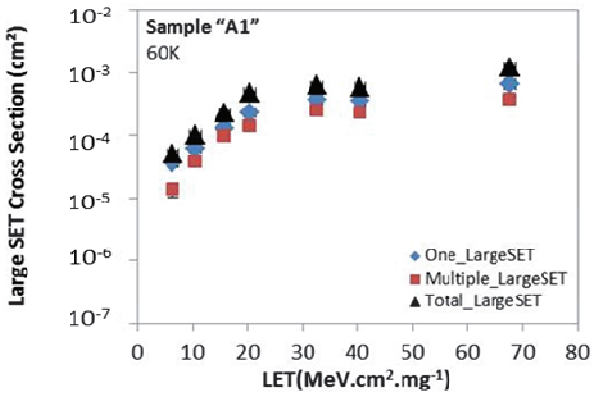

Fig. 7. Large SET experimental cross sections measured on the sample "A1" during the test campaign, as a function of LET at 60K.

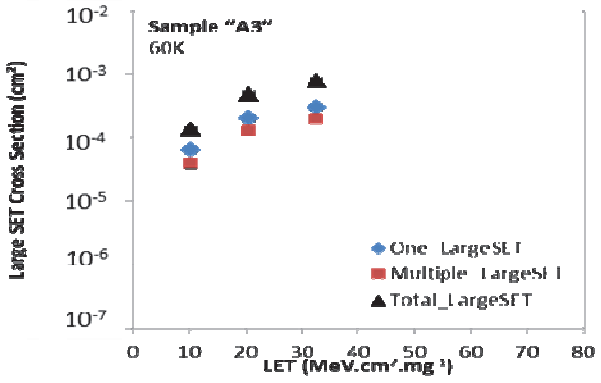

Fig. 8. Large SET experimental cross sections measured on the sample "A1" during the test campaign, as a function of LET at 60K.

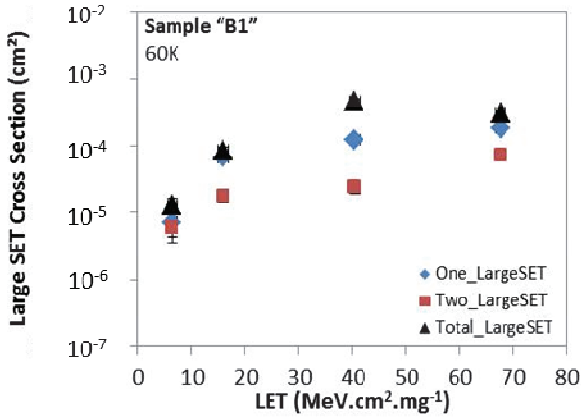

Fig. 9. Large SET experimental cross sections measured on the sample "B1" during the test campaign, as a function of LET at 60K.

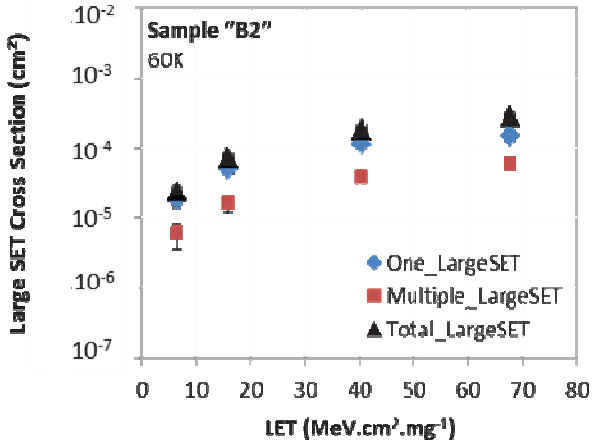

Fig. 10. Large SET experimental cross sections measured on the sample "B2" during the test campaign, as a function of LET at 60K.

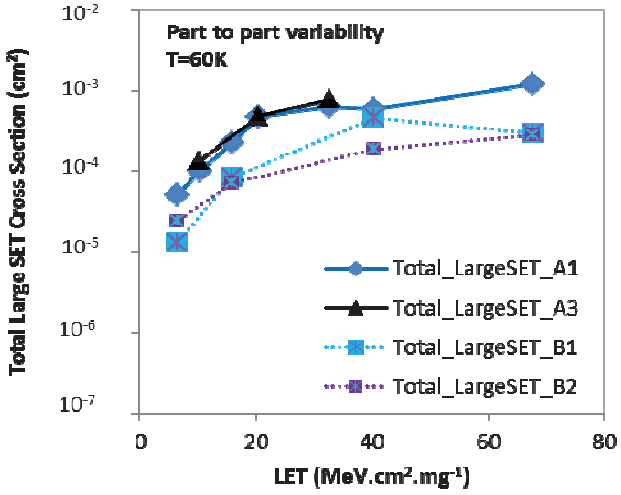

Fig. 11. Total Large SET experimental cross sections measured on the samples "A1, A2, A3, B1, B2" during the test campaign, as a function of LET at 60K.

IV. Discussion

In this section, the SET multiplicity is discussed. Three histograms that represent the occurrence of each SET category for both short and long SET types are presented in section IV.A. This multiplicity origin is investigated in section IV.B by the mean of SEE prediction tool, MUSCA SEP3.

A. Large and Short categories measurements

Fig. 12 presents a histogram of large SET events depending on their multiplicity. Each bar of the histogram represents the number of large SET events on the sample "A1" during test campaign at 60K. It has been irradiated at a fluence 1.10^6.cm^{-2} with a heavy ion LET of about 32MeV.cm^2.mg^{-1}. As mentioned, the ROIC A contains three pixel arrays. The dimensions of the first array are 224 x 4 pixels.

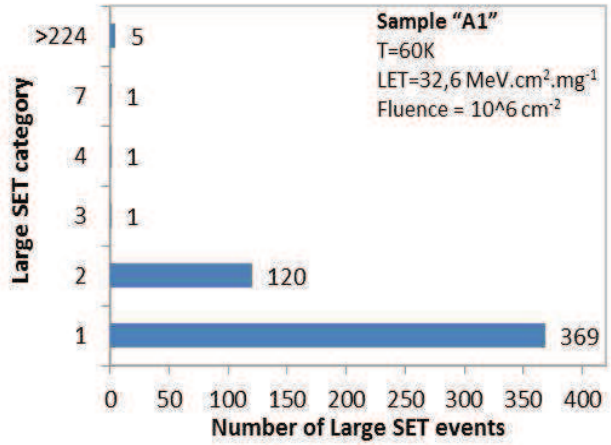

Fig. 12. Number of Large SET events in each categories measured on the sample "A1" during the test campaign at 60K under heavy ion beam, fluence=10^6 .cm^{-2}, LET=32MeV.cm^2.mg^{-1}.

(line x column). The second array is based on 224 x 4 pixels. The third array is based on 448 x 4 pixels. In this histogram, the single large SET events are the main events observed. The number of double large SET (120) is lower by a factor of three than the simple large SET numbers (369). Fig. 12 shows the low probability to observe more than two events on the neighborhood of a pixel. But the event with the seven multiple events during a single video frame seem to be not due to the strike of a heavy ion on the pixel arrays. In this histogram the category of events higher than 224 (the lower column size of pixel tables) is considered as complex SET events. The SEFI sensitivity of the two ROIC designs has been also presented in paper [10]. Two categories of SEFI have been shown: SEFI on the VIDEO frame and SEFI on a multiplexer which is used to control the phase of VIDEO signal. It seems that the design of the multiplexer and its configuration register is more sensitive to SEFIs for the ROIC "B" (NIR detector) than the ROIC "A" (IR detector). This difference in the SEFI sensitivity is highlighted by the LET threshold which is

increased by a factor of 2. Finally, the limited temperature dependence of the SEFI video sensitivity of the two ROIC designs has been shown. The global SEFI sensitivities of the two ROIC are low and compliant with the Sofradir requirements [10].

Fig. 13 presents a histogram of short SET events depending on their multiplicity. Each bar of the histogram represents the number of short SET events on the sample "A3" during test campaign at 60K while it has been irradiated at a fluence $1.10^6.cm^{-2}$ with a heavy ion with a LET of about $32MeV.cm^2.mg^{-1}$. As mentioned this sample contains three pixel arrays which have been described previously. In this histogram, the single short SET events are the main events observed. Two multiple short SET were observed, in two (category '2') and three (category '3') adjacent pixels as shown in Fig. 13. Fig. 13 shows the poor probability to observe more than one short SET on the neighborhood of a pixel. As previously, the events with the multiplicity higher than three during a single video frame does not seem to be due to the strike of a heavy ion on the pixel arrays and are considered as complex short SET. This same observation seems to strengthen the origin of the SETs. In this histogram the category of events higher than 224 (the lower column size of pixel tables) is considered as complex SET events.

A last observation of multiple short SETs is presented in Fig. 14. As previously, each bar of the histogram represents the number of short SET events on a sample of the ROIC B. During the test campaign at 60K, the device has been irradiated with a fluence of $1.10^6.cm^{-2}$ with a heavy ion with a LET of $32.6MeV.cm^2.mg^{-1}$. As the difference of ROIC A, ROIC B contains three pixel arrays with the following dimensions: the first pixel array is 224 x 8 (Line x column).

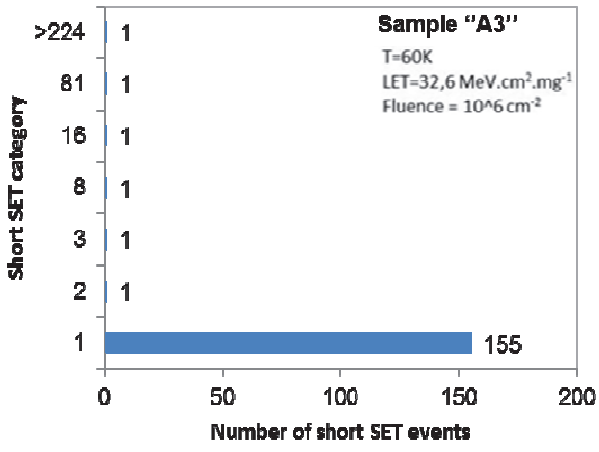

Fig. 13. Number of short SET events in each categories measured on the sample "A3" during the test campaign at 60K under heavy ion beam, fluence=10^6 .cm^{-2}, LET=32.6MeV.cm^2.mg^{-1}.

The second and third arrays are 112 x 4 pixels. In this histogram, the single short SETs events are the only events observed and that confirm the first observation of single short SET in Fig. 13. But, no multiple short SETs were observed, only SEFI events were observed as shown in Fig. 14.

Finally, in order to confirm the hypothesis of the origin of the multiplicity of short and large SET an analysis has been performed by the mean of simulation based on the Monte Carlo SEE prediction tool, MUSCA SEP3. This analysis is presented in the next section.

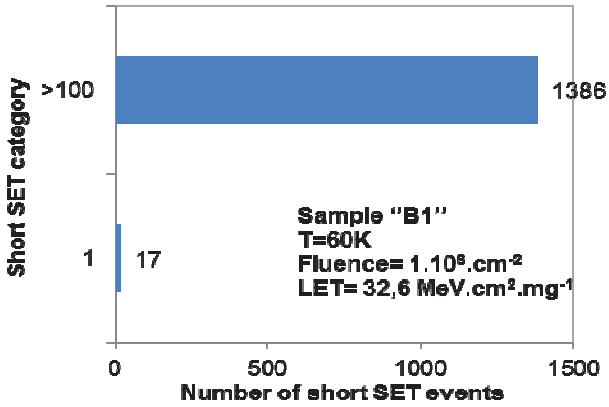

Fig. 14. Number of short SET events in each categories measured on the sample "B1" during the test campaign at 60K under heavy ion beam, fluence=10^6 .cm^{-2}, LET=32.6MeV.cm^2.mg^{-1}.

B. *Analysis Of SET Sensitivity trends by simulations*

SEE prediction tools are used to analyze experimental data and confirm the hypotheses of the SEE experimental trends [5] [6]. Based on the design parameters of the pixel table provided by Sofradir, the SET sensitivity of the ROIC has been calculated.

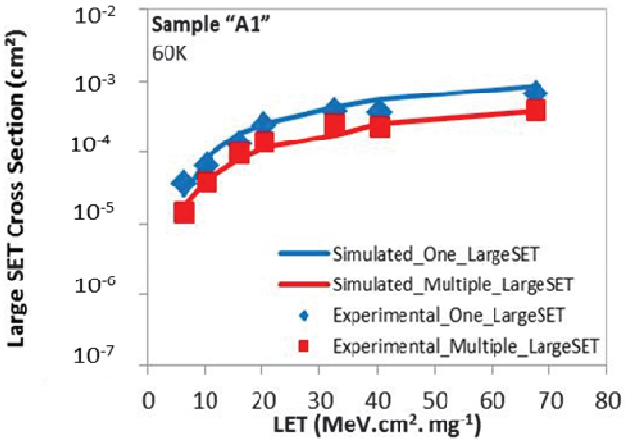

Fig. 15. Large SET experimental and simulated cross sections measured on the sample "A1", as a function of LET at 60K.

Fig. 15 presents the SET cross sections calculated for sample "A1" under heavy ions. The multiplicity of the SET events is highlighted and it confirms that only two SET could be induced by a single particle in the pixel table for this technology. It means that the origin of events higher

than four is due to events on the readout circuit, such as in a DFF of a line or column decoders of the pixel table.

V. Conclusions and perspectives

The SET sensitivity of two readout integrated circuits of infrared image sensor designed by Sofradir is investigated in this paper. Experimental data of short and large SETs obtained for a large range of temperature from 50K up to 300K under a heavy ions beam are presented and analyzed. The temperature impact on the SET cross sections is also presented. The results highlight a limited temperature dependence of the SET susceptibility of the two ROICs. The global SET sensitivities of the two ROIC are low and compliant with Sofradir requirements. The results also highlight a limited impact of the part to part variability in the same lot on the occurrence of SET susceptibility at cryogenic temperature for the ROIC "A" and ''B''. The multiplicity of short SET is lower than of large SET (by a factor of two decades). The multiplicity of the short and large SET events is investigated and analyzed by means of histograms of the short and large SET multiplicity. The two categories of multiplicity have been identified depending on the event location: occurrence one up to four SETs is due to an event in the pixel array, while a SEE occurrence with a higher SET multiplicity is due to an event on an adjacent control circuit. This analysis has been confirmed by simulations performed with the SEE simulation tool MUSCA SEP3.

VI. Acknowledgment

The authors would like to thank TRAD for their support during heavy ions irradiations at UCL facility.

References

[1] G. R. Hopkinson, "Radiation effects in CMOS active pixel sensor," IEEE Trans. Nucl. Sci., vol. 47, no. 6, pp. 2480–2484, Dec. 2000.

[2] C. Virmontois, A. Toulemont, G. Rolland, A. Materne, V. Lalucaa, V. Goiffon, C. Codreanu, C. Durnez, and A. Bardoux, "Radiation-induced dose and single event effects in digital CMOS image sensors,"IEEE Trans. Nucl. Sci., vol. 61, no. 6, pp. 3331–3340, Dec. 2014.

[3] D. Truyen, J. Boch, B. Sgnes, N. Renaud, E. Leduc, S. Arnal, F. Saigne, "Temperature Effect on Heavy-Ion Induced Parasitic Current on SRAM by Device Simulation: Effect on SEU Sensitivity" *, IEEE Trans. Nucl. Sci,* vol. 54, no. 4, pp. 1025-1029, Aug. 2007.

[4] M.J. Gadlage, J. R. Ahlbin, B. Narasimham, B. L. Bhuva, L. W. Massengill, and R. D. Schrimpf, "Single Event Transient measurements in nMOS and pMOS transistor in a 65nm bulk CMOS technology at elevated temperatures", *IEEE, Trans. Device Mater. Reli.*, vol. 11, no. 1, pp. 179-186, Mar. 2011

[5] L. Artola , G. Hubert, « Modeling of elevated temperatures impact on single event transient in advanced CMOS logics beyond the 65-nm technological node », *IEEE Trans. Nucl. Sci*., vol. 61, no. 4, pp. 1611-1617, Aug. 2014.

[6] L. Artola, G. Hubert, O. Gilard, S. Ducret, F. Perrier, M. Boutillier, P. Garcia, G. Vignon, B. Baradat, and Nicolas Ricard," Single Event Upset Sensitivity of D-Flip Flop of Infrared Image Sensors for Low Temperature Applications Down to 77 K", *IEEE Trans. Nucl. Sci*., vol. 62, no. 6, pp. 2979 – 2987, Dec. 2015.

[7] G. Hubert, S. Duzellier, C. Inguimbert, C. Boatella-Polo, F. Bezerra, and R. Ecoffet, "Operational SER calculations on the SAC-C orbit using the multi scales single event phenomena predictive platform (MUSCA SEP3)," *IEEE Trans. Nucl. Sci.,* vol. 56, no. 6, pp. 3032–3042, Dec. 2009

[8] G. Hubert and L. Artola, "Single-event transient modeling in a 65-nm bulk CMOS technology based on multi-physical approach and electrical simulations," *IEEE Trans. Nucl. Sci*., vol. 60, no. 6, pp. 4421–4429, Dec. 2013.

[9] A. Al Youssef, L. Artola, S. Ducret, G. Hubert, F. Perrier, « Investigation of electrical latchup and SEL mechanisms at low temperature for applications down to 50K », *IEEE Trans. Nucl. Sci*., vol. 64, no. 8, pp. 2089-2097, Aug. 2017.

[10] L. Artola, A. Al Youssef, S. Ducret, R. Buiron, S. Parola, G. Hubert, C. Poivey, "Complex Single Event Effects in CMOS pixel selection table and readout integrated circuit dedicated for Infrared Image Sensors" *IEEE Radiation Effects* Data Workshop (REDW) 2017.

[11] M. J. Gadlage, R. J. Ahlbin, V. Ramachandran, P. Gouker, C. A. Dinkins, B. L. Bhuva, B. Narasimhan, R. D. Schrimpf, M. W. Mc- Curdy, M. L. Alles, R. A. Reed, M. H. Mendenhall, L. W. Massengill, R. L. Shuler, and D. McMorrow, "Temperature dependence of digital single-event transients in bulk and fully-depleted soi technologies," *IEEE Trans. Nucl. Sci.*, vol. 56, no. 6, pp. 3115–3121, Dec. 2009.

[12] S. M. Sze and K. K. Ng, Physics of Semiconductor Devices, 3rd ed. Hoboken, N J, USA: Wiley, Nov. 2006.